Controlling conductivity by quantum well states in ultrathin Bi(111) films

P. Kröger,[1] D. Abdelbarey,[1] M. Siemens,[1] D. Lükermann,[1] S. Sologub,[2] H. Pfnür,[1,3,*] and C. Tegenkamp[1,3,4,†]

[1]*Institut für Festkörperphysik, Leibniz Universität Hannover, Appelstraße 2, 30167 Hannover, Germany*

[2]*Institute of Physics, National Academy of Sciences of Ukraine, Nauky Avenue 46, 03028 Kyiv, Ukraine*

[3]*Laboratory of Nano and Quantum Engineering (LNQE), Leibniz Universität Hannover, Schneiderberg 39, 30167 Hannover, Germany*

[4]*Institut für Physik, Technische Universität Chemnitz, Reichenhainer Strasse 70, 09126 Chemnitz, Germany*

(Received 25 October 2017; published 3 January 2018)

Epitaxial Bi(111) films were subject to many and partly even controversial studies on the semimetal-semiconductor transition triggered by a robust quantum confinement. The residual conductance was ascribed to conducting surface channels. We investigated ultrathin crystalline Bi films on Si(111) as a function of film thickness d between 20 and 100 bilayers by means of electric transport measurements. Varying temperature and magnetic field, we disentangled two transport channels. One remains indeed metallic at all thicknesses investigated and exhibits a slightly increasing conductance as a function of d, whereas the second is activated with a d^{-1} dependence of the activation energy, indicating a quasiharmonic confining potential. Both channels reflect the electronic properties of the entire film and do not allow us to strictly separate surface and bulk states. While there is clearly no bulk conductivity, the activated channel is consistently described as electronic excitation into the partly occupied quantum well states, which are also responsible for the metallic conductance and preferentially located close to both interfaces of the film.

DOI: 10.1103/PhysRevB.97.045403

I. INTRODUCTION

The semimetal Bi is characterized by strong spin-orbit coupling and a large Fermi wavelength for bulk electrons, which is around 30 nm. While symmetry prevents spin-orbit split bands in the bulk, surfaces states are strongly spin polarized, and the long Fermi wavelength leads to pronounced quantum confinement effects in thin Bi films [1–9]. Moreover, the Bi(111) films were analyzed recently with respect to their topological character. While few layers of Bi on Si(111) and Bi_2Te_3 were proposed to mimic a quantum spin Hall insulator [10,11], also 30-nm-thick films and even Bi(111) crystals reveal signatures of a nontrivial surface-band dispersion [12,13].

The mesoscopic Fermi wavelength triggered an intense search for a semimetal-semiconductor (SMSC) transition, predicted 50 years ago by Sandormirskii [1]. Using thin Bi films or Bi nanorods, controversial results were obtained [14]. A critical thickness of 30 nm was deduced from magnetotransport experiments with the finding that thinner films become semiconducting in the sense of an SMSC transition [15]. Photoemission results as a function of film thickness were interpreted as evidence that the bulk states indeed undergo the SMSC transition [8]. However, for thin films below 30 bilayers (12 nm) a crossing of the bulk valence band with the Fermi energy was observed, so that the interior of film becomes metallic. This re-entry of the bulk metallicity was explained by surface-state size effect and the accompanied charge transfer between surface and bulk [8].

This interpretation is partly at variance with other measurements. Even below the critical thickness of 12 nm the electronic transport of thin Bi films is always characterized by an activated channel, visible at higher temperature [9] and an additional robust metallic channel at low temperature [9,16,17]. The strong spin-orbit coupling gives rise to a large Rashba splitting for the metallic states [5]. However, this splitting in turn depends on the film thickness, thus demonstrating the close entanglement of all states and questioning the strict separation into bulk and surface states for thin films [18,19].

In this study we performed surface sensitive transport measurements on Bi(111) films grown epitaxially on Si(111). The systematic variation of film thickness and substrate quality allowed us to clearly separate activated from metallic contributions and their relative size. Both transport channels vary as a function of the film thickness, supporting a model with vanishing activation energy in the limit of an infinitely thick film and a remaining metallic state. In other words, this limit corresponds to a semimetallic bulk and a metallic surface state. However, due to quantum-mechanical interaction across the whole film, these states hybridize particularly close to Fermi level and the surface state is rather a partially occupied quantum well state (QWS) defined by the entire film.

II. EXPERIMENTAL SETUP

The transport measurements were performed on Bi films grown on low-doped Si(111) samples ($>1000\,\Omega\,\mathrm{cm}$) of $15 \times 15 \times 0.5$ mm^3 size, hosting four slits and eight $TiSi_2$ contacts under ultrahigh vacuum conditions. Details about the fabrication of contacts as well as the *in situ* cleaning procedures are described elsewhere [20]. Epitaxial Bi films were grown via molecular beam epitaxy at 200 K followed by annealing to 450 K for several minutes. The morphologies of the Si substrates and Bi(111) films were checked by low-energy

*pfnuer@fkp.uni-hannover.de

†christoph.tegenkamp@physik.tu-chemnitz.de

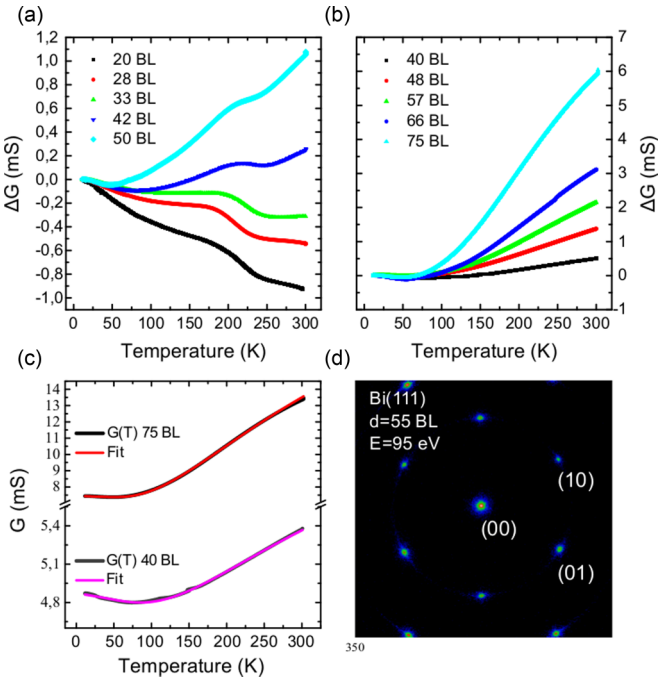

FIG. 1. (a),(b) Conductance as a function of temperature for variously thick Bi(111) films. While for (b) the films were prepared on fresh Si(111) substrates, in (a) the Si(111) templates were used for multiple deposition experiments and high-temperature annealing cycles. (c) $G(T)$ curves for 40- and 75-BL-thick films together with fits according to Eq. (1). (d) LEED pattern of a 55-BL-thick Bi film.

electron diffraction (LEED). A representative LEED image for an epitaxial Bi(111) film is shown in Fig. 1. We used the rhombohedral notation for indexing the Bi planes, i.e., the surface normal coincides with the ⟨111⟩ direction [3]. The layer thickness of the Bi films is given in bilayers (BL $= 1.14 \times 10^{15}$ atoms/cm^2). The Bi coverage was calibrated by recording bilayer oscillations in conductance during the homoepitaxial growth of Bi on Bi(111) films at 10 K. In the course of the project we found that aging of the Si(111) samples is a severe problem. Therefore, the Si samples were flash-annealed in total only a few times. Usually after the fifth deposition experiment we exchanged the Si samples.

III. RESULTS AND DISCUSSION

High quality Bi(111) films were grown by the procedures described above, as obvious from the LEED pattern shown in Fig. 1(d), which is characterized by low background and no indication for rotational disorder. The change of dc conductance as a function of temperature is shown in Figs. 1(a)–1(c) for various film thickness between 20 and 75 BLs. Starting from low temperatures, the conductance first drops for all film thicknesses, which is a hallmark for metallic band transport. A second nonlinear positive contribution to conductance can be identified, which increases with the layer thickness and as a function of temperature. It dominates conductance for film thicknesses above 40 BLs at temperatures above 100 K.

These Bi film specific fingerprints of conductance are highly sensitive to the exact conditions of film preparation and to interface properties. While nonannealed films, though crystalline, show no metallic contribution, frequent removal of the Bi layers by thermal desorption alter film quality of newly prepared films and strongly modify and increase the activated contribution to conductance. The small peak around 180 K, seen in Fig. 1(a), is independent of layer thickness, but increases by repeated thermal desorption of Bi. Since traces of it can also be seen in conductance of bare Si(111) after repeated removal of Bi layers, it is most likely due to an activation of a small concentration of Bi-induced defects within the space charge layer of Si close to the interface [21]. It is not seen for layers grown on a new sample [Fig. 1(b)]. Therefore, it has been neglected in the analysis described below. These defects also deteriorate the growth conditions of the Bi film and yield space charge and impurity-driven transport channels through the Si. In this contexts also impurities from the residual gas may play a role. It was already shown in former studies that high-temperature annealing (>1300 K) leads to the formation of SiC interstitial defects, which severely alters the band bending close to the surface and subsequently increasing the space charge layer contribution [22–24]. Therefore, we flash annealed the Si templates for the Bi films only a few times in order to reduce Si-based interface currents to a minimum.

In order to obtain more quantitative results, we parametrized and fitted the conductance G of the Bi films of thickness d as a function of temperature T, following Ref. [14]:

$$G(T) = \left[G_0^{-1} + aT\right]^{-1} + G_1 \exp\left(-\frac{E_g}{2k_B T}\right); \qquad (1)$$

k_B denotes the Boltzmann factor, and a is a constant. The first term describes the metallic transport (G_0 refers to the conductance at 0 K) including electron-phonon scattering, while the second term accounts for thermally excited carriers. Thereby, G_1 comprises details of the density of states available for activated transport and depends on the carrier concentration and their electronic mobility. The associated quantum size effect induced band gap E_g rather mimics an *effective* gap defined by the energy difference between occupied and (partially) unoccupied states [18]. In former studies, the metallic and activated contributions were synonymously used for surface state and bulk state triggered transport, respectively. We will show below that this assignment is rather suitable in the limit of a semi-infinite Bi(111) film, but is misleading in the case of thin films. The quality of the fit, based on this simple metallic surface and activated bulk transport model, is shown exemplarily for 40- and 75-BL-thick Bi films in Fig. 1(c).

We first discuss the activated transport channel. The energy gaps E_g for the different film thicknesses d, deduced from fitting the data, are plotted in Fig. 2(a) for a wide thickness range. We plotted in total three different series of data and the data follow nicely a $1/d$ behavior. The $1/d$ thickness dependence is confirmed by independent angle-resolved photoemission spectroscopy (ARPES) measurements in the thickness range from 5 to 25 BLs [18]. The extrapolation of ARPES data together with DFT calculations on free-standing Bi films to the film thicknesses here show even quantitative agreement [25].

A $1/d$-thickness behavior is expected for a parabolic confinement potential of the electrons propagating along the ⟨111⟩ direction. This deviation from the generally assumed square well potential [14] is not unexpected in systems with

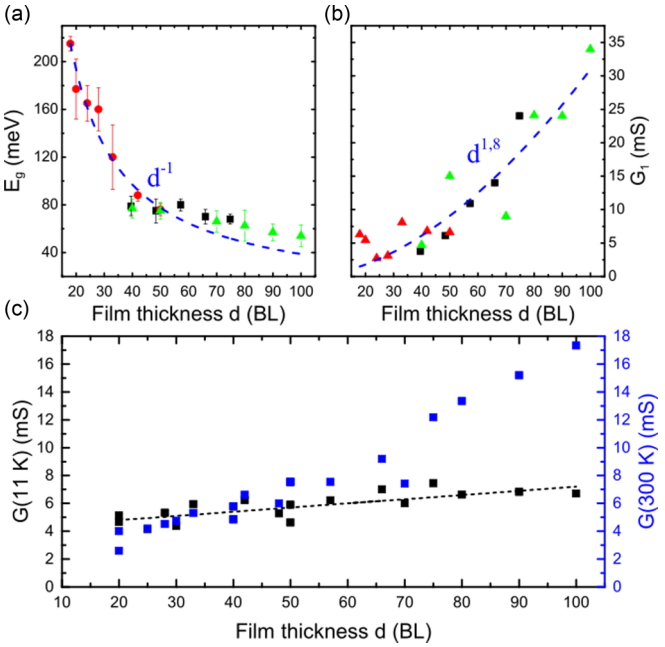

FIG. 2. Energy gap E_g (a), film conductance G_1 (b), and surface conductance G_0 (c) as a function of film thickness. The symbols denote measurements done on different Si(111) surfaces. The color coding in (a) and (b) illustrates sets of measurements performed with different Bi films prepared on the same Si substrate.

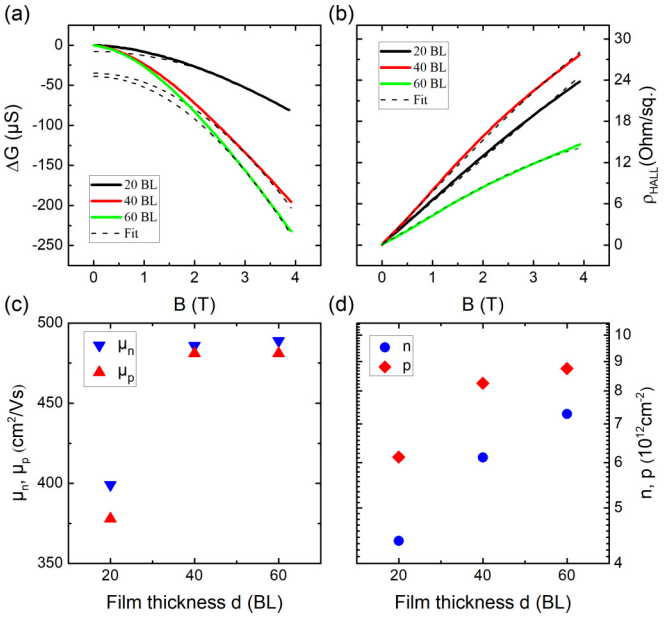

FIG. 3. Magnetotransport results: (a) $G(B)$ and (b) Hall measurements at 11 K. (c) Electron (μ_n) and hole mobilities (μ_p). (d) Electron (n) and hole (p) carrier concentrations as a function of the film thickness.

low charge densities and is quite common for epitaxial films. E.g., for SiO_2 and InSb films exponents of 1.56 and 1.4 were reported [26,27]. Most importantly, E_g is not vanishing even for extremely thin films in accordance with low-temperature transport measurements [9]. However, this finding contrasts with conclusions made from recent APRES experiments, where it was shown that the valence bands at the $\overline{\Gamma}$ point intersects the Fermi level for films below 30 BLs, thus the film should reveal a higher conductance below the critical thickness [8], which is not seen in our transport experiments.

As obvious from Fig. 2(b), the conductance G_1 increases almost quadratically as a function of the film thickness. Note that G_1 should be constant in the case of a film thickness independent bulk band dispersion. Therefore, the pronounced thickness dependence is a direct consequence of the quantum well state formation within the Bi film. A thickness dependence with an exponent close to 2 can be rationalized: the two-dimensional density of states for quantum well split states scales with the size of energy splitting. Moreover, the confinement along the growth direction changes the curvature of the bands, in accordance with high-resolution ARPES measurements [16]. This also widens the k space available for an efficient excitational transfer, roughly with the same exponent.

The metallic conductance at low temperatures (11 K), shown in Fig. 2(c), reflects basically G_0, which is associated with the metallic surface transport channel. Obviously the surface contribution increases linearly with d by around 20% between 20 and 100 BLs [Fig. 2(c)]. We will show below that this effect is governed by the increase of the carrier concentrations and mobilities within the metallic states, as already seen before by transport [17]. The measurements of the total conductance measured at 300 K show a similar behavior as G_1, which supports our assignment from above. Qualitatively, the increase of G_1 reflects the change of the density of states of the bulk valence band as a consequence of the formation of quantum well states within the Bi(111) films.

The $G(T)$ measurements discussed so far were utilized in order to demonstrate the presence of a metallic and activated transport channel. At low temperatures, the contributions from the activated part can be almost neglected and the conductance is governed mainly by the metallic channel. In order to reveal the band mobilities and carrier concentrations we performed magnetotransport measurements at low temperatures. The spin-orbit interaction results in the formation of hole- and electronlike states, that are partially filled [16]. Therefore, at least a two-band model must be used to describe the Bi(111) surface states, which averages over concentrations and mobilities of electrons and holes in the respective bands. The conductance G as a function of the magnetic field B follows

$$G(B) = G(0)\frac{1 + (1-c)^2 \frac{\mu_n^2 \mu_p^2}{(\mu_n + c\mu_p)^2} B^2}{1 + \mu_n \mu_p \frac{\mu_p + c\mu_n}{\mu_n + c\mu_p} B^2}, \qquad (2)$$

where $c \equiv p/n$ denotes the ratio of the hole and electron concentration and $\mu_{n,p}$ the corresponding charge-carrier mobilities [28]. The quadratic behavior is nicely seen in Fig. 3(a), particularly for larger magnetic fields. For small fields the magnetic length $l_H = \sqrt{\hbar/eB}$ is large compared to the film thickness, i.e., in this regime localization effects are important. We will not consider this quantum transport regime further, but want to mention that this contribution was carefully subtracted (see, e.g., [6]).

The Hall resistivity is given by [28]

$$\rho_H(B) = -\frac{B}{ne}\frac{\mu_n^2 - c\mu_p^2 + (1-c)\mu_n^2\mu_p^2 B^2}{(\mu_n + c\mu_p)^2 + (1-c)^2\mu_n^2\mu_p^2 B^2}. \quad (3)$$

Characteristic curves for 20-, 40-, and 60-BL-thick films are shown in Fig. 3(b). To achieve a self-consistent fit, both $G(B)$ and $\rho_H(B)$ were analyzed by using the same set of parameters for a given film thickness. In addition, the dc conductance G (cf. Fig. 2) and the Hall conductance $G_H = \pi/\ln(2)e(n\mu_n + p\mu_p)$ are connected via $G_H = r_H G$, where r_H is the Hall factor. Under the constraint of $r_H = 1$ a reliable determination of all transport parameters for variously thick films is possible. The results for the mobilities and carrier concentrations are shown in Figs. 3(c) and 3(d), respectively.

Most strikingly, the surface conductivity and carrier concentration increases with increasing film thickness, in agreement with the dc conductance discussed in the context of Fig. 2(c). This finding is a hallmark that the surface channel is hybridizing with the bulk. Ideally, for a surface state of a quasi-semi-infinite Bi(111) crystal, i.e., where the thickness d is large compared to the Fermi wavelength, the carrier concentrations remain constant with $c \equiv 1$. For thinner films this ratio deviates and is a measure for the entanglement between the surface and bulk properties [8,17] in this quantum confined state.

Also the carrier mobilities increase with film thickness. From the systematic analysis of the full width at half maximum of the (00)-order spot as a function of the electron energy, i.e., scattering phase, we deduced an average grain size of 50 nm, which was not depending on the film thickness. Thus, also the increase of the carrier mobilities is rather an effect of a modification of the band structure and/or may be due to reduction of quantum coupling between the interfaces as a function of thickness, which reduces the scattering probabilities of the charge carriers.

All these results indicate strong entanglement of states that are usually termed "surface" and "bulk" states. The strong coupling of electronic states located preferentially closer to the interface with those located more in the interior of the film is evidenced by first-principle calculations done for free-standing Bi(111) films. Here the changes of the partially occupied part of the band structure depends sensitively on the number of layers [29], which are thus coupled to the appearance of different quantum well states in these thin films for different film thicknesses. The alleged surface state in a thin Bi(111) film is given by the highest occupied QWS, which strongly hybridizes with the bulk states. Compared to the occupied QWS the partially occupied state shows a pronounced Rashba splitting, which already points towards a location of the QWS close to the interface where the inversion symmetry is clearly broken, in agreement with quantitative calculations [16,29].

The gradual change of the Fermi surface as a function of the film thickness, as seen recently by ARPES [8], points in the same direction, but it turns out to be difficult to clearly resolve the states at Fermi, as the error bars are relatively large. This is most likely the reason why the conclusions drawn from these measurements are partly at variance with former surface transport measurements [17,30] and the conclusions of this work. Based on transport data, the alleged re-entry of metallicity for a 30-BL-thick film [8] is clearly not seen.

While some properties of the metallic conduction channel were characterized more precisely in this work, there is general agreement [9,14,17,30] that this channel is due to the partially occupied QWS located preferentially at the interfaces. These states, however, are coherently coupled. Changes of coupling as a function of layer thickness leads to an increase of mobilities. For the activated channel, on the other hand, our considerations and results clearly show that this channel cannot be described as bulk conductance. States described as being located mostly in the interior of the film are all fully occupied. The lowest excitations possible involve the partially occupied bands just discussed in context with metallic conduction. Therefore, since the activated channel involves always excitations from fully occupied to partially occupied bands, it can preferentially only enhance conductance in the already existing metallic channel(s). Thus in the usual terms it might be described as bulk-to-surface conductance. Unoccupied bulk bands will only contribute when the gap is sufficiently small, i.e., close to or above 100 BLs.

In conclusion, we presented temperature- and magnetic-field-dependent transport measurements on epitaxial Bi(111) films of different thickness below 100 bilayers. In these quantum confined films only partially occupied bands appear for all thicknesses that are responsible for metallic conductance, which slightly increases with film thickness due to band relaxations and changes of coherent coupling. These highest occupied quantum well states are strongly hybridized in thin films and turn into the surface state for infinite thickness. This interpretation can conclusively explain the different experimental findings for Bi films and Bi nanostructures and identifies the activated conduction channel as bulk-to-surface conduction. Moreover, the topological character found in thin Bi(111) films for the metallic states might be a result of this trivial entanglement between the occupied and metallic QWS. The ideal surface state concept is a result of the broken lattice invariance, which *per se* is not well defined in a film of finite thickness. Therefore, the near-surface transport channel has different properties than the surface state of bulk material, is rather delocalized with respect to the geometric surface of the film, and couples the edges. This interpretation of the films as quantum-mechanical objects can also explain why the interface at the Si(111) surface also revealed a conducting channel and why the film as a whole undergoes a so-called allotropic phase transition [2]. Recently, we performed angle-resolved magnetotransport measurements, which support this conclusion [31].

ACKNOWLEDGMENTS

We gratefully acknowledge the financial support by the Deutsche Forschungsgemeinschaft (Project No. Pf238/31) and by DAAD.

[1] V. Sandomirkii, Sov. J. Exp. Theor. Phys. Lett. **25**, 101 (1967).
[2] T. Nagao, J. T. Sadowski, M. Saito, S. Yaginuma, Y. Fujikawa, T. Kogure, T. Ohno, Y. Hasegawa, S. Hasegawa, and T. Sakurai, Phys. Rev. Lett. **93**, 105501 (2004).

[3] M. Kammler and M. H. von Hoegen, Surf. Sci. **576**, 56 (2005).
[4] P. Hofmann, Prog. Surf. Sci. **81**, 191 (2006).
[5] T. Hirahara, K. Miyamoto, I. Matsuda, T. Kadono, A. Kimura, T. Nagao, G. Bihlmayer, E. V. Chulkov, S. Qiao, K. Shimada *et al.*, Phys. Rev. B **76**, 153305 (2007).
[6] D. Lükermann, S. Sologub, H. Pfnür, C. Klein, M. Horn-von Hoegen, and C. Tegenkamp, Phys. Rev. B **86**, 195432 (2012).
[7] C. Klein, N. J. Vollmers, U. Gerstmann, P. Zahl, D. Lükermann, G. Jnawali, H. Pfnür, C. Tegenkamp, P. Sutter, W. G. Schmidt *et al.*, Phys. Rev. B **91**, 195441 (2015).
[8] T. Hirahara, T. Shirai, T. Hajiri, M. Matsunami, K. Tanaka, S. Kimura, S. Hasegawa, and K. Kobayashi, Phys. Rev. Lett. **115**, 106803 (2015).
[9] K. Zhu, L. Wu, X. Gong, S. Xiao, and X. Jin, Phys. Rev. B **94**, 121401 (2016).
[10] M. Zhou, W. Ming, Z. Liu, Z. Wang, P. Li, and F. Liu, Proc. Natl. Acad. Sci. USA **111**, 14378 (2014).
[11] T. Hirahara, G. Bihlmayer, Y. Sakamoto, M. Yamada, H. Miyazaki, S.-i. Kimura, S. Blügel, and S. Hasegawa, Phys. Rev. Lett. **107**, 166801 (2011).
[12] M.-Y. Yao, F. Zhu, C. Q. Han, D. D. Guan, C. Liu, D. Qian, and J.-F. Jia, Sci. Rep. **6**, 21326 (2016).
[13] Y. Ohtsubo, L. Perfetti, M. O. Goerbig, P. L. Fèvre, F. Bertran, and A. Taleb-Ibrahimi, New J. Phys. **15**, 033041 (2013).
[14] S. Xiao, D. Wei, and X. Jin, Phys. Rev. Lett. **109**, 166805 (2012).
[15] C. A. Hoffman, J. R. Meyer, F. J. Bartoli, A. Di Venere, X. J. Yi, C. L. Hou, H. C. Wang, J. B. Ketterson, and G. K. Wong, Phys. Rev. B **48**, 11431 (1993).
[16] T. Hirahara, T. Nagao, I. Matsuda, G. Bihlmayer, E. V. Chulkov, Y. M. Koroteev, P. M. Echenique, M. Saito, and S. Hasegawa, Phys. Rev. Lett. **97**, 146803 (2006).
[17] D. Lükermann, S. Sologub, H. Pfnür, and C. Tegenkamp, Phys. Rev. B **83**, 245425 (2011).
[18] A. Takayama, T. Sato, S. Souma, T. Oguchi, and T. Takahashi, Nano Lett. **12**, 1776 (2012).
[19] M. Aitani, T. Hirahara, S. Ichinokura, M. Hanaduka, D. Shin, and S. Hasegawa, Phys. Rev. Lett. **113**, 206802 (2014).
[20] C. Tegenkamp, D. Lükermann, S. Akbari, M. Czubanowski, A. Schuster, and H. Pfnür, Phys. Rev. B **82**, 205413 (2010).
[21] N. N. N. Riemann, H. Abrosimov, ECS Trans. **3**, 53 (2006).
[22] T. Hirahara, I. Matsuda, C. Liu, R. Hobara, S. Yoshimoto, and S. Hasegawa, Phys. Rev. B **73**, 235332 (2006).
[23] H. M. Zhang, K. Sakamoto, G. V. Hansson, and R. I. G. Uhrberg, Phys. Rev. B **78**, 035318 (2008).
[24] F. Edler, I. Miccoli, J. P. Stöckmann, H. Pfnür, C. Braun, S. Neufeld, S. Sanna, W. G. Schmidt, and C. Tegenkamp, Phys. Rev. B **95**, 125409 (2017).
[25] T. Hirahara, T. Nagao, I. Matsuda, G. Bihlmayer, E. V. Chulkov, Y. M. Koroteev, and S. Hasegawa, Phys. Rev. B **75**, 035422 (2007).
[26] C. Ke, W. Zhu, Z. Zhang, E. Soon Tok, B. Ling, and J. Pan, Sci. Rep. **5**, 17424 (2015).
[27] K. Berchtold and D. Huber, Phys. Status Solidi B **33**, 425 (1969).
[28] A. B. Pippard, *Magnetoresistance in Metals* (Cambridge University Press, Cambridge, England, 1989).
[29] Y. M. Koroteev, G. Bihlmayer, E. V. Chulkov, and S. Blügel, Phys. Rev. B **77**, 045428 (2008).
[30] T. Hirahara, I. Matsuda, S. Yamazaki, N. Miyata, S. Hasegawa, and T. Nagao, Appl. Phys. Lett. **91**, 202106 (2007).
[31] P. Kroeger, C. Tegenkamp, and H. Pfnür (unpublished).